ADVANCED FUNCTIONAL MATERIALS
www.afm-journal.de

Foam-Like Behavior in Compliant, Continuously Reinforced Nanocomposites

*Brent J. Carey, Prabir K. Patra, Myung Gwan Hahm, and Pulickel M. Ajayan**

In the pursuit of advanced polymer composites, nanoscale fillers have long been championed as promising candidates for structural reinforcement. Despite progress, questions remain as to how these diminutive fillers influence the distribution of stresses within the matrix and, in turn, influence bulk mechanical properties. The dynamic mechanical behavior of elastomer-impregnated forests of carbon nanotubes (CNTs) has revealed distinct orientation-dependent behavior that sheds light on these complicated interactions. When compressed along the axis of the fillers, the composite will mimic open-cell foams and exhibit strain softening for increasing amplitudes due to the collective Euler buckling of the slender nanotubes. In contrast, the same material will behave similarly to the neat polymer when compressed orthogonal to the alignment direction of the nanotubes. However, in this orientation the material is incapable of achieving the same ultimate compressive strain due to the role that the embedded nanotubes play in augmenting the effective cross-link density of the polymer network. Both of these responses are recoverable, robust, and show little dependency on the diameter and wall-number of the included CNTs. Such observations give insight into the mechanics of polymer/nanoparticle interactions in nanocomposite structures under strain, and the thoughtful control of such coordinated buckling behavior opens the possibility for the development of foam-like materials with large Poisson ratios.

1. Introduction

Due to their impressive material properties,[2] carbon nanotubes (CNTs) have been explored for a wide variety of applications. When utilized as the primary reinforcement in composites, many questions still remain as to how their presence truly influences the mechanical response of the resultant material.[1] Such concerns are critical in the pursuit of lightweight, multifunctional composites,[3,4] and while incompatibility between the two phases does offer the potential for great mechanical damping,[5,6] efforts have been made to improve load transfer across the matrix/filler interface by functionalizing CNTs with moieties that are chemically compatible with a desired matrix.[7] Similarly, considerable progress has been made in understanding how the presence of a nanoparticle influences a polymer's morphology, with regard to concepts such as transcrystallinity[8,9] and the formation of an "interphase" where the polymer's conformity is distinctly different than the bulk matrix.[10,11] To this day, however, the precise interactions between nanoscale fillers and a matrix material under even modest deformations are not completely understood.

For the purposes of mechanical reinforcement, an oft-overlooked attribute of these polymeric macromolecules[12] is their remarkable ability to recover elastically from high-strain deformations.[13,14] CNTs with modest aspect ratios have been modeled[15] and experimentally demonstrated[16] to either kink or buckle symmetrically about their central axis when loaded, resulting in a limit point instability that leads to a negative slope in the stress vs. strain relationship. This "negative stiffness" behavior has been exploited for extreme mechanical damping,[17] and also in the development of composite materials whose strength supersedes the rule of mixtures.[18] In contrast, high aspect ratio CNTs will buckle as near-ideal Euler columns when compressed axially.[16]

As with individual nanotubes, it has been shown experimentally[19,20] and through finite element modeling[21] that self-assembled arrays of multi-walled CNTs (MWNTs) can recover from numerous compressive cycles. The practical limitation of this is that the CNT architecture will plastically deform beyond some threshold strain.[22] Similar nanotube forests have been impregnated by several matrix polymers including polystyrene[23] and poly(methylmethacrylate),[24] and by introducing a compliant, elastic matrix such as poly(dimethylsiloxane) (PDMS),[25] this bed of springs can be supported to allow for high-cycle recoverability. The compression of a material with such a high degree of filler orientation has yielded distinct orientation-dependent deformation modes, allowing for the experimental isolation of behavior that assists in the fundamental understanding of how nanoscale fillers influence the bulk properties of nanocomposite materials.

Dr. B. J. Carey, Dr. M. G. Hahm, Prof. P. M. Ajayan
Department of Mechanical Engineering & Materials Science
Rice University
Houston, TX 77005, USA
E-mail: ajayan@rice.edu
Prof. P. K. Patra
Departments of Mechanical Engineering
and Biomedical Engineering
University of Bridgeport
Bridgeport, CT 06604, USA

DOI:10. 1002/adfm.201201999

2. Anisotropic Dynamic Mechanical Response

Through the precise control of amplitude, frequency, and temperature during cyclic deformation, dynamic mechanical analysis (DMA) can yield subtle micromechanical information. For compression transverse to the alignment direction of few-walled CNTs (FWNTs; **Figure 1**) as well as many-walled MWNTs (Supporting Information Figure SI-1), it is revealed that the stiffness is nonlinear up to a 4% strain amplitude, followed by a linear region of deformation from 4% to 6% strain. From 6% to 10% strain the trend is evocative of what is seen in the 10% to 14% strain range of the neat polymer. Aside from the higher stiffness, the strain-dependent response of the composite resembles the trend of the pure PDMS with a lower ultimate compressive strain (an observation that is further supported by the stress/strain relationship in Figure 1b). Conducting strain sweeps for several frequencies, Figure SI-2 (Supporting Information) demonstrates that the neat polymer and the radially stressed FWNT composite are consistent between.5 Hz and 10 Hz.

The similarities in mechanical response became even more apparent when the materials were subjected to various input parameters. Frequency sweeps from.5 Hz to 100 Hz were conducted at several amplitudes, and the data was compiled into a 3D surface plot to reveal the landscape of resonances for each material. While stiffness (Figure SI-3, Supporting Information) provided some binsight, the damping (tan δ) proved much more effective for the purposes of comparison. It is qualitatively observed that the topography of the radially stressed FWNT (**Figure 2**) and MWNT (Figure SI-4, Supporting Information) composite surface plots (i.e., the position and intensity of peaks and troughs) bear a strong resemblance to the neat

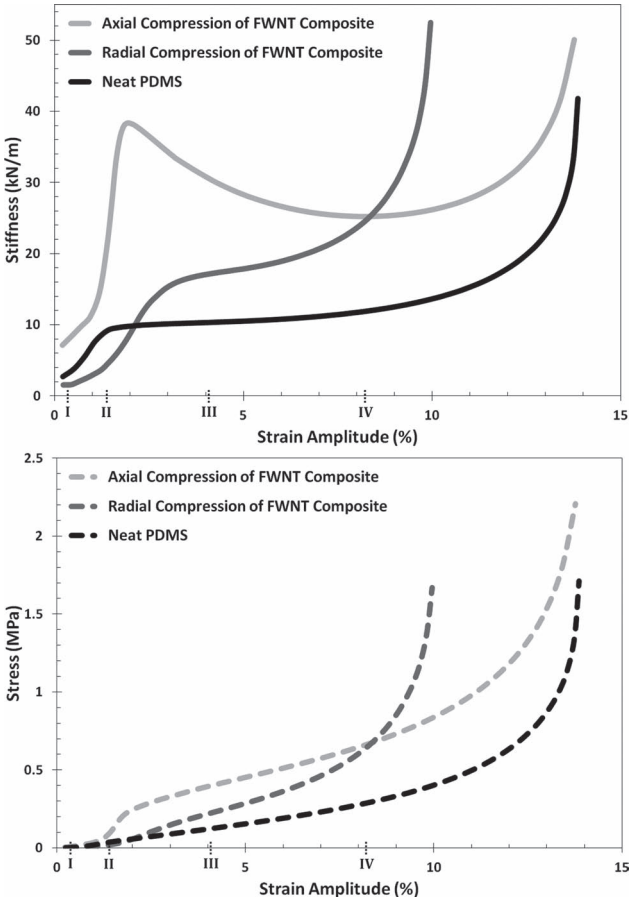

Figure 1. The dynamic mechanical response of continuously reinforced CNT/PDMS composites. The a) stiffness and b) stress for various strain amplitudes reveal that elastomer-impregnated forests of FWNTs will exhibit strongly anisotropic behavior when subjected to cyclic uniaxial compression. The composite performs similarly to the neat polymer when tested transverse to the alignment direction of the nanotubes, yet with a much lower ultimate compressive strain. Compression along the axis of the FWNTs, however, reveals a distinct dynamic strain softening response that is strikingly similar to what is observed in open-cell foams. These observations are mirrored for MWNTs (Figure SI-1, Supporting Information) and shed light on the mechanics of deformation in compliant nanocomposite materials.

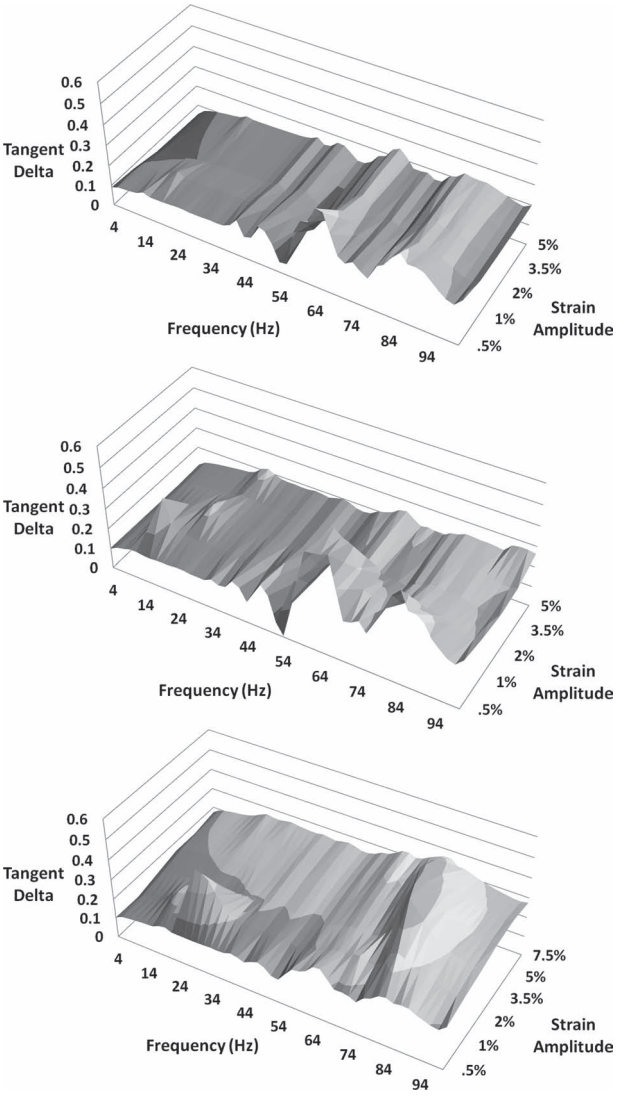

Figure 2. Comparing the mechanics of deformation through viscoelasticity. The behavior of the a) neat polymer is qualitatively determined to be quite similar to the b) radially stressed CNT composite over a broad range of amplitudes and frequencies, suggesting similar mechanics of deformation. Conversely, the c) axially compressed composite responds quite differently, indicating that the mechanics of deformation are markedly different in this orientation.

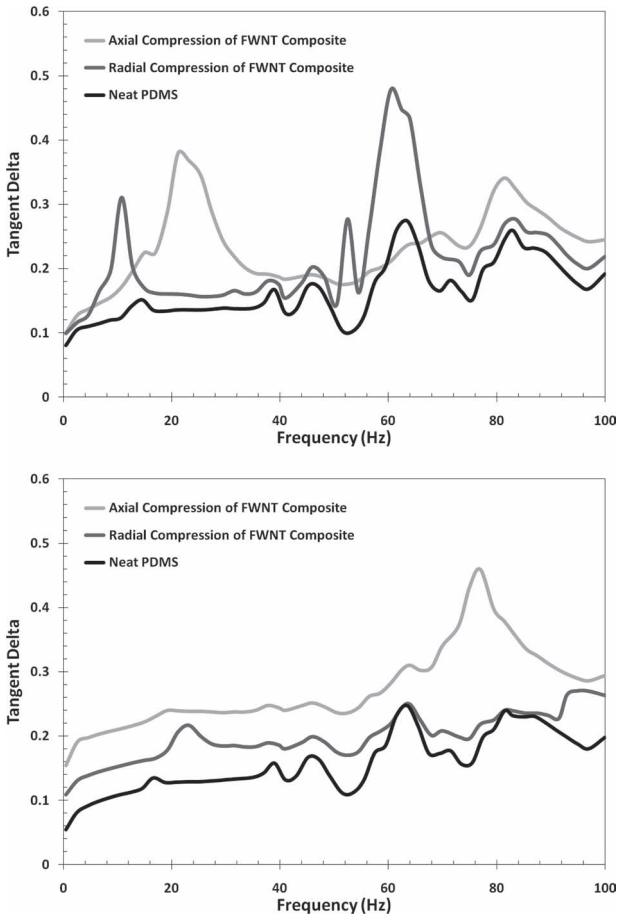

Figure 3. Closer inspection of frequency dependencies. By comparing the low- and high-strain frequency sweeps from Figure 2, subtleties of deformation become apparent. a) The compressive resonance of the highly aligned CNTs in the axial sample is believed to contribute to the 22 Hz resonance at 1% strain, yet this peak has disappeared for b) 5% strain amplitudes where a resonance at 78 Hz resonance has emerged. While the resonances in the pure polymer are not predominant in the composite samples for small amplitudes, similarities emerge for large-amplitude compression.

polymer, providing further evidence that the mechanics of deformation are similar when the composite is compressed in this orientation.

There is, however, some discrepancy below a 2% strain amplitude, where several of the resonances are amplified for the composite. Selecting frequencies below (1%) and above (5%) the 2% threshold, we observe in **Figure 3** that the 61 Hz resonance in PDMS is greatly amplified in the radially stressed composite for low amplitudes, and that all resonances are muted for greater amplitudes. It is difficult to conclusively index the 61 Hz resonance, though the orientation of the CNTs offers some insight. Shear stress at the filler/matrix interface has been implicated in mechanical damping for nanocomposite materials,[6] and it is conceivable that this event corresponds to geometrical resonance longitudinal to the alignment direction of the nanotubes.

In contrast to the radial deformation, the composite responds quite differently from the neat polymer when loaded along the axis of the CNTs. This is immediately evident in Figure 1a and Figure SI-1a (Supporting Information), where the dynamic stiffness of the composite is similar up to a 1% strain amplitude before spiking rapidly at 2% strain to a four-fold improvement over the neat polymer. This then leads to a regime where further increases in the amplitude of oscillation will induce a reduction in stiffness, a response known as dynamic strain softening. Beyond a 9% strain amplitude, the stiffness will increase rapidly in a manner that is reminiscent of the neat polymer, ultimately achieving the same ultimate compressive strain (14%).

The FWNT (Figure 2c) and MWNT (Figure SI-4c, Supporting Information) surface plots also suggest dissimilar mechanics of deformation, as the topography is observably different than the unfilled polymer over a wide range of frequencies and amplitudes. Despite this dissimilar behavior, the stress-strain relationship in Figure 1b shows a familiar trend for moderate to high amplitudes. In other words, in the absence of the anomaly at ≈2% strain, the plot of the axially deformed composite would almost exactly coincide with that of the pure polymer.

An assessment of the low-strain frequency sweep (Figure 3a) reveals a resonance at 22 Hz that does not appear to originate from the polymer. This resonance completely disappears for greater amplitudes (Figure 3b), where another emerges at 78 Hz. Across the entire range of frequencies, it is seen that the axial composite and neat polymer resonance profiles differ substantially for low amplitude oscillation, yet bear some resemblance to each other for larger amplitudes. Collectively, these observations suggest a shift in the mechanics of deformation for strain amplitudes greater than 2%.

3. Understanding the Mechanics of Deformation

To explain these orientation-dependent responses, it is important to understand the source of viscoelasticity in vulcanized rubbers. Elastomer networks experience such impressive compliancy due to the ability of the limber polymer chains to translate as they stretch and elongate, and the idealized mechanics of deformation in the neat polymer correspond to the Roman numerals in Figure 1. Only the shortest elements of the network bear load for low-amplitude oscillations (I), leading to a nonlinear region (II) that extends until all elements of the network are being engaged (III). The linear region of deformation that follows will continue until elements of the network begin to reach full extension (IV). Given the absence of a distinct CNT signature in the strain- and frequency-dependent response of the radially stressed composite, it is expected that the mechanics of deformation in this orientation closely match the neat polymer.

An understanding of the forest impregnation process provides some additional perspective. During infiltration, the polymer will navigate around the coaxially oriented CNT filaments, displacing air and filling the interstitial space. The ends of the individual chains will cross-link as the polymer cures, resulting in a highly compliant network that is intertwined with the preferentially aligned nanotubes. Viscoelastic analysis from previous work indicates that there is no shift in the glass transition (T_g) due to the presence of the CNTs, suggesting

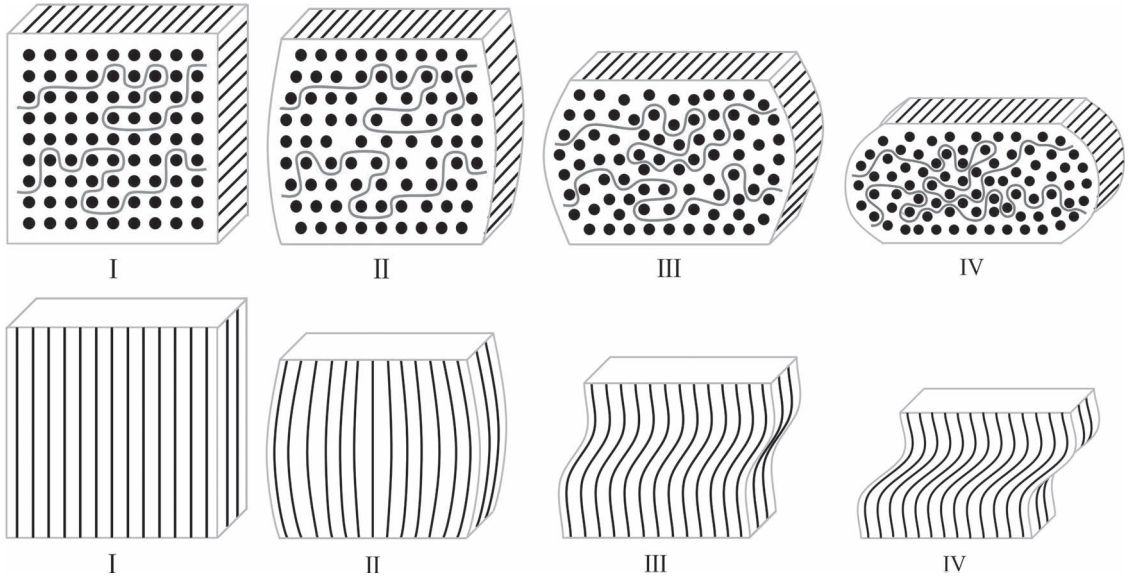

Figure 4. Proposed mechanics of deformation for continuously reinforced compliant nanocomposites. a) Translation of the preferentially oriented nanotubes (black dots; into the page) during radial compression would produce a response identical to the neat polymer, and their separation during loading would expedite the full extension of the elements of the elastomer network (red lines). b) For axial deformation, a transition from the typical barreling behavior to the collective Euler buckling of the nanotube struts (vertical lines) would explain the dynamic strain hardening and similarity to foams, despite the absence of a cellular microstructure.

that there is little-to-no chemical interaction between the two phases and no alteration of the cross-link density of the polymer matrix.[26]

For low-amplitude compressive deformation normal to the nanotube alignment direction, it is expected that the polymer will increasingly engage the aligned CNTs for greater amplitudes. The growing stress will pressure the separation of the nanotubes as the sample bulges outward (a process known as "barreling"). Such deformation mechanics, illustrated in **Figure 4**a, would neatly explain why the radially stressed composite responds similarly to the pure polymer and shows no clear signature of the nanotubes. The ultimate compressive strain would understandably be lower for such a mechanism, as the rod-like CNTs would increase the effective cross-link density of the matrix by serving as pulleys that expedite the full extension of the polymer network. In Figure 4a, the example polymer chain is meant to represent an individual element in the three-dimensional polymer network (i.e., a PDMS chain between one or more nodes).

In contrast, the mechanics of deformation are clearly much different when compressing along the axis of the CNTs. Dynamic strain softening is known to occur in filled elastomers–a response known as the Payne effect–due to the breakage and re-forming of physical bonds at the matrix/filler interface for polymer chains that span between filler particles.[27] For the material in the present work however, the trends below (<2%) and above (>9%) the softening regime are not typical of traditional filled rubber systems. The absence of the Payne effect in this composite is perhaps due to the continuous reinforcement provided by the high aspect ratio CNTs (as opposed to particulate fillers), though the root cause for this aberration is not immediately clear. In any case, the disparity suggests that a different mechanism is responsible.

In accordance with what has been observed in anisotropic MWNT/polymer composites prepared through mechanical mixing and extrusion,[28] it was believed that CNT kinking or microstructural buckling might be responsible. While it has been reported that negatively stiff cylindrical inclusions can be stabilized by a positively stiff elastomer coating or matrix,[29] the work of Yap, Lakes, and Carpick provides strong evidence that nanotubes of a sufficiently large aspect ratio will buckle, yet never kink.[16]

Forests of CNTs have been shown to exhibit two distinct modulus regions when compressed,[19] and can reversibly compress to less than 15% of their free height though the formation of neat, self-organized folds.[20] This behavior is likened to the mechanics of open-cell foams, where the modeling of nonlinear deformation has demonstrated that columnar constitutive elements will buckle during uniaxial compression.[30] Such deformation is possible since these materials have low Poisson ratios (spanning between 0 and 0.5, this ratio represents the degree of volumetric change during loading, as measured by the transverse strain during uniaxial deformation). Curiously, despite the presence of the PDMS matrix (Poisson ratio: 0.5) between the CNTs to eliminate the previous cellular/porous structure, the stress-strain relationship of the axially deformed composite is strikingly similar to such foams.[31]

Based on these determinations, it is believed that the axially stressed composite will transition from barreling below a 2% strain amplitude to the collective Euler buckling of the nanotube struts for larger amplitudes of deformation. Such a transition, as illustrated in Figure 4b, neatly explains the dynamic strain softening behavior and agrees with the various experimental observations.

The pre- and post-buckled state of the CNTs would contribute to the polymer-independent resonances at 22 Hz in Figure 3a

and 78 Hz in Figure 3b, respectively. Further, the "spring-like" contribution of the buckled nanotubes would account for the step increase in the stress-strain relationship (Figure 1b) and divergence in stiffness for various frequencies (Figure SI-2b, Supporting Information) beyond a 2% strain amplitude.

Moreover, the collective recovery of these struts at the offset of loading would explicate the high-strain and high-frequency recoverability of the axially loaded composite as compared to the other samples and loading orientations. In the absence of a matrix, forests of CNTs have been shown to recover at a rate greater than 2 mm/s.[20] A close examination of Figure SI-3 (Supporting Information) reveals that, 1) only the axially stressed composites were able to achieve a 7.5% strain amplitude at 100 Hz and 2) the dynamic strain softening is quite robust and will occur up to frequencies in excess of 100 Hz.

Such a long-range coordinated deformation mechanism also would provide a sensible explanation for the composite's ability to achieve the same ultimate compressive strain as the neat polymer, despite the presence of high-aspect-ratio inclusions. Coordinated buckling would mitigate transverse strains until the point where the elastomer network would otherwise reach full extension. In a sense, achieving the ultimate compressive strain in this orientation is analogous to the process of densification in foams.

In accordance with the Euler buckling of freestanding columns, it is expected that the buckling mode of this composite is some function of the boundary conditions. Given that the Q800 DMA has one fixed platen and one that can deflect laterally, the requisite solution of Euler's buckling formula yields a sinusoid with a period of $L/2$, as represented in the schematic. Lastly, while this anisotropic response is seen in the FWNT and MWNT composites alike, it is observed that the behavior of the FWNT is much more distinct. This is likely due to the greater degree of nanotube orientation and tighter distribution of diameters in such forests (as seen in Supporting Information Figure SI-5).

4. Conclusions

In summary, we have presented the unusual and highly anisotropic dynamic mechanical behavior of a continuously aligned, elastomer-impregnated nanocomposite. Compressed transverse to the axis of the carbon nanotube reinforcements, the composite responds quite similarly to the neat polymer, yet with a notably lower ultimate compressive strain. In this orientation, the high-aspect-ratio nanotubes effectively increase the cross-link density of the elastomer network during deformation. The response of the composite is distinctly different when compressed along the axis of the CNTs, and its dynamic stiffness will decrease as a function of an increasing amplitude of oscillation. This dynamic strain softening behavior is strongly reminiscent of open-cell foams, despite the lack of any cellular structure and a proximate Poisson ratio of 0.5, and is attributed to the collective Euler buckling of the CNTs within the polymer matrix. Such observations provide insight into the interactions between nanomaterials and a surrounding polymer, while also revealing unusual mechanical responses with promising practical utility.

5. Experimental Section

Nanotube Synthesis: The FWNTs (5–12 nm in-diameter) and MWNTs (ranging broadly from 50–100 nm in-diameter) were synthesized via water-assisted ethylene chemical vapor deposition (CVD) with a 1.5 nm pre-deposited Fe catalyst,[32] and vapor-phase CVD with xylene and ferrocene precursors,[33] respectively. As described elsewhere, the forests contain ≈5% CNTs by volume.[25]

Composite Preparation: The as-grown forest of FWNTs are not able to withstand the force exerted by the monomer during impregnation, and it was necessary to anchor the tips of the FWNTs in a PDMS/FWNT/PDMS sandwich structure prior to infiltration.[34] Otherwise, the infiltration procedure is identical to the MWNT composites, as shown earlier, with the polymer completely displacing the interstitial air between the CNTs.[25] All samples were hand-cut approximately 2.5 mm long × 1 mm wide × 1 mm thick to allow for the radial and axial testing of an individual sample.

Strain Sweeps: Using a TA Instruments Q800 DMA, each sample was subjected to uniaxial compression for a range of strain amplitudes up to its own specific elastic limit. All sweeps (0.5 Hz, 1 Hz, 2 Hz, 5 Hz, 7.5 Hz, and 10 Hz) were conducted at room temperature, and were repeated 5 times to ensure reproducibility. The 5 Hz sweeps are featured in Figure 1 and Figure SI-1 (Supporting Information).

Frequency Sweeps: Again using the Q800, each sample was tested at room temperature for various distinct strain amplitudes encompassing the elastic limit of the polymer (0.5%, 1%, 2%, 3.5%, 5%, 7.5%). Each sample was swept from.05 Hz to 100 Hz, repeating each cycle a total of 5 times. The results were composited into 3D surface plots to represent the frequency- and strain-dependent responses of each material and testing orientation.

Supporting Information

Supporting Information is available from the Wiley Online Library or from the author.

Acknowledgements

The authors would like to acknowledge the NASA Graduate Student Researchers Program (GSRP) for financial support.

Received: July 17, 2012
Revised: November 14, 2012
Published online: January 16, 2013

[1] E. T. Thostenson, C. Li, T.-W. Chou, *Compos. Sci. Technol.* **2005**, *65*, 491.
[2] A. Jorio, M. S. Dresselhaus, G. Dresselhaus, *Carbon Nanotubes: Advanced Topics in the Synthesis, Structure, Properties and Applications*, Springer, Berlin **2008**.
[3] P. M. Ajayan, J. M. Tour, *Nature* **2007**, *447*, 1066.
[4] H. D. Wagner, R. A. Vaia, *Mater. Today* **2004**, *7*, 38.
[5] J. N. Coleman, U. Khan, W. J. Blau, Y. K. Gun'ko, *Carbon* **2006**, *44*, 1624.
[6] J. Suhr, N. Koratkar, *J. Mater. Sci.* **2008**, *43*, 4370.
[7] A. Eitan, K. Jiang, D. Dukes, R. Andrews, L. S. Schadler, *Chem. Mater.* **2003**, *15*, 3198.
[8] R. Haggenmueller, J. E. Fischer, K. I. Winey, *Macromolecules* **2006**, *39*, 2964.
[9] S. Zhang, M. L. Minus, L. Zhu, C.-P. Wong, S. Kumar, *Polymer* **2008**, *49*, 1356.
[10] T. Ramanathan, H. Liu, L. C. Brinson, *J. Polym. Sci., Polym. Phys.* **2005**, *43*, 2269.

[11] K. W. Putz, M. J. Palmeri, R. B. Cohn, R. Andrews, L. C. Brinson, *Macromolecules* **2008**, *41*, 6752.
[12] M. J. Green, N. Behabtu, M. Pasquali, W. W. Adams, *Polymer* **2009**, *50*, 4979.
[13] M. R. Falvo, G. J. Clary, R. M. Taylor, V. Chi, F. P. Brooks, S. Washburn, R. Superfine, *Nature* **1997**, *389*, 582.
[14] B. I. Yakobson, C. J. Brabec, J. Bernholc, *Phys. Rev. Lett.* **1996**, *76*, 2511.
[15] J. Feliciano, C. Tang, Y. Zhang, C. Chen, *J. Appl. Phys.* **2011**, *109*, 084323.
[16] H. W. Yap, R. S. Lakes, R. W. Carpick, *Nano Lett.* **2007**, *7*, 1149.
[17] R. A. Ibrahim, *J. Sound Vib.* **2008**, *314*, 371.
[18] T. Jaglinski, D. Kochmann, D. Stone, R. S. Lakes, *Science* **2007**, *315*, 620.
[19] J. Suhr, V. Pushparaj, L. Ci, S. Sreekala, X. Zhang, O. Nalamasu, P. M. Ajayan, *Nat. Nanotechnol.* **2007**, *2*, 417.
[20] A. Cao, P. L. Dickrell, W. G. Sawyer, M. N. Ghasemi-Nejhad, P. M. Ajayan, *Science* **2005**, *310*, 1307.
[21] S. B. Hutchens, A. Needleman, J. R. Greer, *J. Mech. Phys. Sol.* **2011**, *59*, 2227.
[22] A. A. Zbib, S. D. Mesarovic, E. T. Lilleodden, D. McClain, J. Jiao, D. F. Bahr, *Nanotechnology* **2008**, *19*, 175704.
[23] S. Boncel, K. K. K. Koziol, K. Z. Walczak, A. H. Windle, M. S. P. Shaffer, *Mater. Lett.* **2011**, *65*, 2299.
[24] N. R. Raravikar, L. S. Schadler, A. Vijayaraghavan, Y. Zhao, B. Wei, P. M. Ajayan, *Chem. Mater.* **2005**, *17*, 974.
[25] L. Ci, J. Suhr, V. Pushparaj, X. Zhang, P. M. Ajayan, *Nano Lett.* **2008**, *8*, 2762.
[26] B. J. Carey, P. K. Patra, L. Ci, G. G. Silva, P. M. Ajayan, *ACS Nano* **2011**, *5*, 2715.
[27] A. R. Payne, *J. Appl. Polym. Sci.* **1962**, *6*, 57.
[28] E. T. Thostenson, T.-W. Chou, *Carbon* **2004**, *42*, 3015.
[29] D. M. Kochmann, W. J. Drugan, *J. Mech. Phys. Sol.* **2009**, *57*, 1122.
[30] L. Gong, S. Kyriakides, *Int. J. Solids Struct.* **2005**, *42*, 1381.
[31] J. A. Elliot, A. H. Windle, J. R. Hobdell, G. Eeckhaut, R. J. Oldman, W. Ludwig, E. Boller, P. Cloetens, J. Baruchel, *J. Mater. Sci.* **2002**, *37*, 1547.
[32] L. Ci, R. Vajtai, P. M. Ajayan, *J. Phys. Chem. C* **2007**, *111*, 9077.
[33] R. Andrews, D. Jacques, A. M. Rao, F. Derbyshire, D. Qian, X. Fan, E. C. Dickey, J. Chen, *Chem. Phys. Lett.* **1999**, *303*, 467.
[34] B. Li, M. G. Hahm, Y. L. Kim, H. Y. Jung, S. Kar, Y. J. Jung, *ACS Nano* **2011**, *5*, 4826.